THE ASTROPHYSICAL JOURNAL, 497:294–302, 1998 April 10

THE COOL WHITE DWARF LUMINOSITY FUNCTION AND THE AGE OF THE GALACTIC DISK

S. K. LEGGETT[1,2]
Joint Astronomy Centre, University Park, Hilo, HI 96720
MARÍA TERESA RUIZ[1,2]
Departamento de Astronomía, Universidad de Chile, Santiago, Chile
AND
P. BERGERON[1,2]
Lockheed Martin Canada, 6111 Avenue Royalmount, Montréal, Québec, Canada H4P 1K6
Received 1997 August 1; accepted 1997 November 18

ABSTRACT

We present new optical and infrared data for the cool white dwarfs in the proper motion sample of Liebert, Dahn, & Monet. Stellar properties—surface chemical composition, effective temperature, radius, surface gravity, mass, and luminosity—are determined from these data by using the model atmospheres of Bergeron, Saumon, & Wesemael. The space density contribution is calculated for each star and the luminosity function (LF) for cool white dwarfs is determined. Comparing the LF to the most recent cooling sequences by Wood implies that the age of the local region of the Galactic disk is 8 ± 1.5 Gyr. This result is consistent with the younger ages now being derived for the globular clusters and the universe itself.

Subject headings: stars: evolution — stars: fundamental parameters — stars: luminosity function, mass function — white dwarfs

1. INTRODUCTION

The great majority of stars—all stars formed with an initial mass less than 8 $M_\odot$ and spectral type later than mid-B—will end their lives as electron–degenerate white dwarfs. The white dwarfs are most likely to be composed of a carbon/oxygen core surrounded by a helium envelope and, in some cases, a hydrogen layer on top of the helium layer. Trace metals may also be present. The remnants slowly cool to invisibility with an approximately constant radius. Theoretical cooling curves show that even remnants aged 10 Gyrs (10 Gyrs since ejection of the planetary nebula) will be visible, with luminosities $\sim 10^{-4}\ L_\odot$ and effective temperature ~ 5000 K (Wood 1992). These calculations are supported by observations of cool white dwarfs, which show a well-defined faint limit to the degenerate sequence in color-magnitude diagrams (e.g., Monet et al. 1992). The limit of $M_V \sim 16$ is a direct reflection of the finite age of the disk of the Galaxy. White dwarfs have simply not had enough time to cool to fainter magnitudes. This is not an observational selection effect. Fainter stars could be detected (fainter red dwarfs, for example, have been detected). The fact that we can still see the remnants of the first burst of star formation has led researchers to use the observed luminosity function (LF) of cool white dwarfs as a constraint on the age of the Galaxy (e.g., Winget et al. 1987; Iben & Laughlin 1989; Wood 1992; Oswalt et al. 1996; Salaris et al. 1996). In recent studies, the most commonly used observational LF is that published by Liebert, Dahn, & Monet (1988, hereafter LDM). This LF is based on a sample of 43 spectroscopically confirmed white dwarfs taken from the Luyten Half-Second Catalog (Luyten 1979). Although the LDM sample is well understood, this work suffered, unavoidably, from shortcomings in the model atmospheres available at that time and in the data then available. Both of these restricted the accuracy with which the authors could determine the chemical composition and luminosity of the stars in the sample.

For the last few years we have been conducting an extensive spectroscopic and photometric survey aimed at determining more precise atmospheric parameters for a large sample of cool white dwarfs. In Bergeron, Ruiz, & Leggett (1997, hereafter BRL), we presented new spectroscopic and photometric data for many cool ($T_{\rm eff} < 8000$ K) degenerates and derived accurate values of chemical composition, effective temperature, surface gravity, and hence, radius, mass, luminosity, and cooling age for the stars, by using state-of-the-art model atmospheres by Bergeron, Saumon, & Wesemael (1995). In that paper we also demonstrated and discussed the complex relationship between composition and temperature, and attempted to provide an improved understanding of the chemical evolution of cool white dwarfs. In BRL we refer to the shortcomings in the LDM LF (in particular, the uncertain bolometric corrections) and state that our goal is to improve the determination of the white dwarf LF and the estimate of the age of the local Galactic disk. This is the aim of the present paper. Since the publication of BRL, we have completed the optical and infrared data set for the LDM sample, and these data are presented in § 2. We analyze the data with the models of Bergeron, Saumon, & Wesemael (1995) and present the results of that analysis in § 3. The new LF is presented in § 4, and the implications for the age of the Galaxy are discussed in § 5.

2. OBSERVATIONS

We have obtained optical spectroscopy and optical and infrared photometry, or a subset of these, for the 43 stars in the LDM sample, two of which form an unresolved binary

[1] Visiting Astronomer, Cerro Tololo Inter-American Observatory. CTIO is operated by AURA, Inc. under contract to the National Science Foundation.

[2] Visiting Astronomer, Kitt Peak National Observatory. KPNO is operated by AURA, Inc., under contract to the National Science Foundation.

system in our data set (G107-70A/B). Data for 28 objects in this sample have already been presented in BRL. New data have been obtained since then for the purpose of this analysis, and these data are described here. The optical spectra were obtained with the R-C spectrograph attached to the Cerro Tololo Inter-American Observatory (CTIO) 4 m telescope in 1995 December and with the R-C spectrograph attached to the KPNO 4 m telescope in 1996 May. Optical *BVRI* photometry was obtained in 1996 June with the CCD on the KPNO 0.9 m telescope. The *JHK* infrared photometry was obtained with CIRIM on the CTIO 4 m telescope in 1995 December, NSFCAM on the NASA Infrared Telescope Facility (IRTF) in 1996 February and 1996 August, and IRCAM on the UK Infrared Telescope in 1996 August and 1996 October. Table 1 gives both the earlier results presented in BRL and the new data for 19 stars (the new results are identified by the notes to the Table). In Table 1, column (1) gives the white dwarf number; column (2) the name; column (3)–(4) the trigonometric parallax and error from the Yale Catalogue (van Altena, Lee, & Hoffleit 1994); or Liebert, Dahn, & Monet (1989); column (5) the Hα equivalent width (a value of $W = 0$ implies a featureless spectrum near the Hα region); columns (6)–(9) the *BVRI* data on the Cousins system (Bessell & Weis 1987) with the number of independent observations in column (10); column (11)–(13) the JHK on the CIT system (Elias et al. 1982) with the number of independent observations in column (14). Notes are given in the final column. The photometric uncertainties are 3% at *V*, *R*, and *I*, and 5% elsewhere, unless stated otherwise in the notes.

TABLE 1

OBSERVATIONAL RESULTS

WD (1)	Name (2)	π (mas) (3)	σ_π (mas) (4)	W (Å) (5)	V (6)	$B-V$ (7)	$V-R$ (8)	$V-I$ (9)	N (*BVRI*) (10)	J (11)	$J-H$ (12)	$H-K$ (13)	N (*JHK*) (14)	Notes (15)
0011−134.....	LHS 1044	50.8	5.2	7.15	15.89	0.63	0.33	0.67	1	14.85	0.23	0.10	1	1
0046+051.....	vMa 2	232.5	1.9	0.00	12.39	0.52	0.26	0.49	2	11.69	0.08	0.09	1	2
0145−174.....	LHS 147	14.0	9.2	11.30	17.62	0.35	0.24	0.46	1	17.00	0.06	−0.01	1	3
0208+396.....	G74−7	59.8	3.5	...	14.51	0.33	0.25	0.47	1	13.80	0.15	0.02	1	4
0213+427.....	LHS 153	50.2	4.1	3.64	16.22	0.73	0.45	0.85	1	14.98	0.25	0.21	2	5, 6
0322−019.....	G77−50	...	...	2.39	16.12	0.82	0.46	0.88	2	14.63	0.26	0.09	2	4
0341+182.....	Wolf 219	52.6	3.0	0.00	15.19	0.33	0.28	0.54	1	14.56	0.21	−0.05	1	7
0423+044.....	LHS 1670	...	...	0.53	17.14	1.00	0.54	1.02	2	15.55	0.25	−0.02	2	
0426+588.....	Stein2051B	180.7	0.8	0.00	12.43	0.30	0.26	0.57	1	11.84	0.11	0.05	1	5
0435−088.....	L879−14	105.2	2.6	0.00	13.75	0.33	0.32	0.57	2	13.00	0.15	0.06	1	7
0552−041.....	LP 658−2	155.0	2.1	0.00	14.47	1.01	0.50	0.98	2	13.05	0.15	0.09	3	2
0553+053.....	G99−47	125.1	3.6	8.23	14.16	0.62	0.38	0.75	2	12.96	0.19	0.11	2	1
0659−064.....	LHS 1892	81.0	24.2	8.31	15.43	0.43	0.30	0.60	1	14.58	0.29	0.05	1	5
0727+482.....	G107−70AB	90.0	1.0	...	14.65	0.98	0.53	1.02	1	13.05	0.24	0.09	2	
0738−172.....	L745−46A	112.4	2.7	4.88	13.06	0.24	0.18	0.34	1	12.65	0.03	0.13	2	4, 5
0747+073A.....	LHS 239	54.7	0.7	0.41	16.96	1.21	0.65	1.26	2	15.05	0.15	0.04	2	
0747+073B.....	LHS 240	54.7	0.7	0.00	16.63	1.06	0.58	1.08	2	14.96	0.23	0.01	2	
0802+387.....	LHS 1980	...	...	0.00	16.85	0.96	0.51	1.00	1	15.26	0.24	0.06	1	5
0912+536.....	G195−19	97.0	1.9	0.00	13.84	0.35	0.20	0.33	2	13.22	0.07	0.06	1	5, 8
1022+009.....	LHS 282	...	...	3.19	18.14	0.70	0.43	0.88	1	16.81	0.33	0.12	1	
1033+714.....	LHS 285	...	...	0.00	16.88	1.08	0.55	1.08	1	...	...	...		5
1042+593.....	LHS 291	10.6	5.4	0.00	17.80	0.07	0.27	0.40	2	...	...	...		5, 7
1043−188.....	LHS 290	56.9	6.5	0.00	15.52	0.57	0.49		1	14.62	0.21	0.05	1	5, 9
1055−072.....	LHS 2333	82.3	3.5	0.00	14.33	0.30	0.20	0.42	1	13.81	0.10	0.02	1	5
1108+207.....	LHS 2364	38.3	2.7	0.00	17.70	0.97	0.53	1.07	2	15.91	0.22	0.07	2	
1121+216.....	LHS 304	74.5	2.8	14.00	14.21	0.31	0.20	0.45	1	13.58	0.18	0.00	1	5
1239+454.....	LHS 2596	...	...	9.89	16.50	0.46	0.30	0.61	2	15.47	0.17	0.00	1	5
1247+550.....	LP 131−66	39.5	0.7	0.00	17.79	1.44	0.76	1.45	1	15.72	0.05	0.04	2	
1257+037.....	LHS 2661	60.3	3.8	5.07	15.84	0.66	0.38	0.76	2	14.56	0.23	0.08	2	
1300+263.....	LHS 2673	28.4	3.3	0.00	18.77	1.24	0.68	1.28	2	16.85	0.21	−0.02	1	3, 5, 10
1334+039.....	Wolf 489	121.4	3.4	1.19	14.63	0.95	0.51	1.01	1	13.06	0.26	0.10	2	
1344+106.....	LHS 2800	49.9	3.6	11.60	15.12	0.38	0.22	0.48	1	14.38	0.18	0.01	1	5
1345+238.....	LP 380−5	82.9	2.2	0.46	15.71	1.15	0.59	1.13	2	13.92	0.25	0.08	2	
1444−174.....	LHS 378	69.0	4.0	0.00	16.44	1.03	0.49	1.01	1	14.98	0.14	0.19	1	
1633+572.....	G225−68	69.2	2.5	0.00	14.99	0.50	0.31	0.61	1	14.03	0.06	−0.02	2	5, 9
1748+708.....	G240−72	164.7	2.4	0.00	14.13	0.48	0.53	1.05	1	12.77	0.07	0.20	1	8, 11
1756+827.....	LHS 56	63.9	2.9	12.10	14.34	0.35	0.22	0.47	2	...	...	...		5
2002−110.....	LHS 483	57.7	0.8	0.00	16.95	1.16	0.59	1.09	2	15.32	0.21	0.02	2	5
2054−050.....	vB 11	64.6	5.1	0.00	16.69	1.20	0.66	1.32	1	14.82	0.21	0.07	1	
2248+293.....	G128−7	47.8	4.2	4.70	15.54	0.66	0.40	0.79	1	14.24	0.22	0.06	3	5
2251−070.....	LP 701−29	123.7	4.3	0.00	15.71	1.84	0.61	1.15	2	13.86	0.23	0.16	2	12
2316−064.....	LHS 542	32.2	3.7	0.00	18.15	1.08	0.62	1.16	1	16.40	0.25	0.02	1	5, 10

NOTE.—(1) Magnetic with Zeeman split Hα, (2) Metal-rich DZ, (3) *K* photometry only good to 10%, (4) Hydrogen- and metal-rich DAZ, (5) New data since BRL, (6) *H* and *K* photometry only good to 10% due to nearby bright star, (7) Carbon-rich DQ, (8) Magnetic non-DA based on polarization measurements: Schmidt & Smith 1995, (9) C_2H star (cf. Schmidt et al. 1995), (10) Trigonometric parallax from Liebert, Dahn, & Monet 1989, (11) G240−72 "yellow sag" seen in spectrum, e.g., Wesemael et al. 1993, and (12) LP 701−29 heavily blue blanketed (Dahn et al. 1978).

3. ANALYSIS

Significant improvements have recently been made to the model atmospheres of cool white dwarfs. The improvements to the models include new calculations of the collision–induced H_2 opacity, better treatment of H_3^+ (important for H^- opacity), modeling of pressure ionization of He (important for He^- opacity), and more accurate line-broadening calculations for Hα. These new models are described in detail by Bergeron, Saumon, & Wesemael (1995) and BRL.

Our fitting technique is described in detail by BRL, so we will only summarize the procedures here. The observed magnitudes are converted into a flux averaged over the filter bandpass, and these fluxes are compared to those predicted by the model atmosphere calculations. Initially, a surface gravity of $\log g = 8.0$ is adopted, and the effective temperature and angular diameter (diameter divided by distance to the star) are derived by a least-squares fit. For those stars with available trigonometric parallaxes, the stellar radius is determined from the angular diameter and distance. The evolutionary models by Wood (1990, 1995) are used to derive a mass from the radius and temperature; by knowing a mass and radius, a surface gravity can be calculated and compared to the initial assumption. This process is iterated until agreement is reached on $\log g$. In most cases the final value is very close to 8.0, and the assumption of $\log g = 8.0$ for the stars without measured trigonometric parallaxes is valid.

The dominant chemical composition of the atmosphere can be determined from the fit to the energy distribution. The spectroscopy is only used as an internal check on the photometric solutions, or to derive limits on the abundances. For hydrogen-rich stars, Wood's "thick" envelope models are used (helium mass $10^{-2}M_{\rm WD}$ and hydrogen mass $10^{-4}M_{\rm WD}$) and, for the helium–rich stars, the "thin" models are used (helium mass $10^{-4}M_{\rm WD}$ and no hydrogen). The reader is referred to BRL for examples of fits to the observational data. We can reproduce very well both the observed energy distributions and the Hα profiles with the new models. For H-rich atmospheres, the photometry and Hα allow us to constrain the amount of He present to less than 50%, which has a negligible effect on the derived parameters. For He-rich atmospheres, we can constrain the amount of H present to less than 1%. However, this has a large effect on the derived parameters: $T_{\rm eff}$ would be reduced by 250 K, and $\log g$ would be reduced by 0.15 dex, with an implied reduction in mass of $0.07\ M/M_\odot$, if this much hydrogen were present in the atmosphere (see, e.g., LHS 3917 in Fig. 16 of BRL). Table 2 gives the derived properties of the stars in the sample: effective temperature, radius, $\log g$, chemical composition, mass and age from Wood's evolutionary models, and bolometric magnitude. A space density is also given, which is discussed in § 4.

Errors are given in Table 2. The error in effective temperature is derived directly from the fits to the energy distributions, while the errors of $\log g$ and other quantities have been derived by propagating the error of the trigonometric-parallax uncertainty; for the objects with no parallax measurements and for which we assumed the value of $\log g$, there is no assigned uncertainty except in temperature. For the stars without parallaxes, we have derived distances by obtaining a radius for the star from Wood's models (from the effective temperature and adopted $\log g = 8.0$), which, combined with the measured angular diameter, gives distance. The uncertainty in the envelope mass leads to additional uncertainties in the derived masses $\sim 0.03 M/M_\odot$ and uncertainties in $\log g \sim 0.02$ dex. The effect of varying core composition (e.g., from pure carbon to a carbon/oxygen mix) on the derived mass and gravity is much smaller than varying surface-layer mass (because the core composition does not have a large effect on the mass-radius relationship, see Bergeron, Saffer, & Liebert (1992) and references therein).

We do not explicitly give the luminosity in Table 2, but it can be easily derived from the bolometric magnitude as

$$M_{\rm bol} = -2.5 \log L/L_\odot + 4.75\ , \qquad (1)$$

where the solar luminosity $L_\odot = 3.86 \times 10^{26} W$. The total luminosity of each star is determined by

$$L = 4\pi R^2 \sigma T_{\rm eff}^4\ , \qquad (2)$$

where σ is Stefan's constant. For the stars without parallaxes available, $\log g = 8.0$ is adopted, and the radius is derived from Wood's cooling models, as described above.

The ages in Table 2 are obtained from Wood's models with pure carbon core composition. However, these age estimates depend sensitively on the core composition and the helium layer mass (Wood 1992, 1995). For instance, for the coolest white dwarfs with $\log L/L_\odot \sim -4.4$, the age estimates based on C core models are about 1 Gyr *larger* than those based on C/O core models. The ages could be further reduced by ~ 1.5 Gyr if the helium layers were a hundred times thicker, i.e., $q({\rm He}) = 10^{-2}$, as discussed by Wood (1992, 1995).

3.1. *Stellar Properties*

The largest chemical group of stars in this sample have hydrogen-rich atmospheres and show Hα—16 stars fall into this category, two of which are magnetic with Zeeman-split Hα [LHS 1044 (0011−134) and G99-47 (0553+053), see BRL]. A further two stars are H-rich but too cool for Hα to be detected [LHS 2364 (1108+207) and LP 131−66 (1247+550)]. Thirteen stars hot enough to show Hα are actually featureless and must therefore have He-rich atmospheres. Three of them, however, are best fitted with H-rich atmospheres: (1) G107−70A/B (0727+482) is a known binary (unresolved in our data set), and its combined energy distribution is therefore difficult to interpret; (2) LHS 1980 (0802+387) has a noisy spectrum; and (3) G195−19 (0912+536) is magnetic with a peculiar broad absorption feature seen in the blue. There are two other He-rich stars with broad optical features: (1) G240−72 (1748+708, also magnetic) whose spectroscopic feature has been tentatively identified by BRL as C_2H molecular bands smeared by the presence of the ~ 200 MG magnetic field, and (2) LP 701−29 (2251−070), a DZ star whose spectrum shows strong Ca I and Ca II lines, especially Ca I λ4226, and a strong drop in the flux shortward of ~ 4400 Å (Dahn et al. 1978). There are additional stars in the sample with identifiable metallic features. There are two H-rich DAZ stars [G74−7 (0208+396) and G77−50 (0322−019)], and two He-rich DZ stars [vMa2 (0046+051) and L658−2 (0552−041)]. There is one star that we fitted with an He-rich atmosphere, although it shows Hα and metals [L745−46A (0738−172); see also Sion et al. 1990]; this star is fairly hot (~ 8000 K) and has a helium-dominated atmosphere (see BRL and references therein). Another

TABLE 2

STELLAR PROPERTIES

WD	$T_{\rm eff}$ (K)	R 10^{-3} $R_\odot$	log g	H or He	$M/M_\odot$	Cooling Age (Gyr)	Age (Gyr)[a]	$M_{\rm bol}$	$1/v_{\rm max}$ (10^{-4} pc^{-3})
0011−134	6018 (122)	11.2 (1.1)	8.19 (0.15)	H	0.71 (0.10)	3.74 (1.20)	4.0	14.32 (0.22)	0.395
0046+051	6751 (194)	9.5 (0.1)	8.41 (0.01)	He	0.84 (0.01)	4.66 (0.06)	4.8	14.19 (0.02)	1.082
0145−174[b]	7748 (206)	12.8	8.00	H	0.60	1.23	1.8	12.94	0.004
0208+396	7318 (175)	12.6 (0.7)	8.02 (0.09)	H	0.60 (0.05)	1.46 (0.18)	2.0	13.21 (0.13)	0.325
0213+427	5475 (120)	12.2 (1.0)	8.06 (0.14)	H	0.62 (0.08)	4.29 (1.22)	4.7	14.55 (0.17)	0.281
0322−019[c]	5204 (116)	12.6	8.00	H	0.58	4.67	5.3	14.69	0.585
0341+182	6862 (200)	11.3 (0.6)	8.17 (0.09)	He	0.68 (0.06)	2.69 (0.39)	3.0	14.55 (0.17)	0.190
0423+044	5136 (113)	12.6	8.00	H	0.58	4.91	5.6	14.75	0.192
0426+588	7153 (182)	11.0 (0.1)	8.21 (0.01)	He	0.70 (0.01)	2.54 (0.04)	2.8	13.62 (0.01)	0.993
0435−088	6654 (160)	11.7 (0.3)	8.11 (0.04)	He	0.64 (0.02)	2.74 (0.14)	3.1	13.79 (0.05)	0.755
0552−041	5082 (64)	10.2 (0.2)	8.33 (0.02)	He	0.78 (0.01)	8.09 (0.07)	8.2	15.29 (0.03)	0.632
0553+053	5789 (113)	11.1 (0.3)	8.20 (0.04)	H	0.72 (0.03)	4.53 (0.36)	4.7	14.51 (0.06)	3.787
0659−064	6527 (150)	7.5 (2.5)	8.71 (0.37)	H	1.05 (0.22)	4.52 (0.65)	4.6	14.85 (0.62)	1.669
0727+482[d]	4900 (83)	18.2 (0.2)	7.35 (0.02)	H	0.27 (0.01)	2.00 (0.05)	...	14.16 (0.03)	0.764
0738−172[e]	7968 (133)	10.8 (0.2)	8.23 (0.04)	He	0.72 (0.02)	2.00 (0.10)	2.2	13.18 (0.05)	1.648
0747+073A[f]	4166 (81)	15.4 (0.2)	7.65 (0.02)	H	0.39 (0.01)	4.72 (0.21)	...	15.22 (0.03)	0.066
0747+073B	4871 (54)	12.1 (0.2)	8.05 (0.02)	He	0.60 (0.01)	6.85 (0.26)	7.4	15.07 (0.03)	0.066
0802+387[g]	5071 (116)	12.6	8.00	H	0.58	5.14	5.8	14.80	0.339
0912+536[h]	7196 (195)	10.2 (0.2)	8.30 (0.03)	He	0.77 (0.02)	3.16 (0.21)	3.3	13.74 (0.04)	0.558
1022+009	5351 (119)	12.7	8.00	H	0.58	4.13	4.8	14.57	0.016
1033+714	4888 (80)	12.5	8.00	He	0.57	6.09	6.8	14.99	0.030
1042+593	8339 (452)	12.6	8.00	He	0.58	1.34	2.0	12.66	0.001
1043−188	6220 (212)	11.9 (1.4)	8.08 (0.18)	H/He	0.62 (0.11)	3.15 (1.02)	3.6	14.05 (0.24)	0.054
1055−072	7453 (203)	9.2 (0.4)	8.45 (0.06)	He	0.87 (0.04)	3.73 (0.35)	3.8	13.82 (0.10)	2.337
1108+207	4644 (160)	12.1 (0.8)	8.07 (0.12)	H	0.63 (0.08)	7.29 (0.99)	7.7	15.28 (0.16)	0.236
1121+216	7496 (185)	11.1 (0.4)	8.21 (0.06)	H	0.73 (0.04)	1.91 (0.22)	2.1	13.39 (0.09)	0.813
1239+454	6390 (140)	12.7	8.00	H	0.59	1.99	2.6	13.78	0.119
1247+550[i]	4000 (65)	16.5 (0.3)	7.52 (0.04)	H	0.33 (0.01)	4.12 (0.22)	...	15.25 (0.04)	0.066
1257+037	5597 (107)	11.4 (0.7)	8.16 (0.10)	H	0.69 (0.06)	4.86 (0.89)	5.1	14.60 (0.14)	0.559
1300+263	4539 (50)	10.8 (1.2)	8.23 (0.17)	He	0.72 (0.11)	9.46 (0.84)	9.7	15.63 (0.25)	0.085
1334+039	5048 (116)	12.9 (0.3)	7.96 (0.06)	H	0.56 (0.03)	4.79 (0.50)	5.6	14.77 (0.06)	0.005
1344+106	7114 (170)	11.9 (0.8)	8.10 (0.11)	H	0.66 (0.07)	1.79 (0.35)	2.1	13.46 (0.16)	0.410
1345+238	4688 (142)	13.9 (0.4)	7.85 (0.05)	H	0.49 (0.02)	4.96 (0.42)	7.9	14.94 (0.06)	0.397
1444−174	4989 (63)	9.6 (0.6)	8.40 (0.08)	He	0.83 (0.05)	8.52 (0.13)	8.6	15.49 (0.13)	0.459
1633+572	6098 (207)	12.1 (0.5)	8.06 (0.06)	H/He	0.61 (0.04)	3.17 (0.34)	3.6	14.10 (0.08)	0.178
1748+708	5626 (94)	9.6 (0.1)	8.39 (0.02)	He	0.83 (0.01)	6.76 (0.06)	6.9	14.94 (0.03)	2.260
1756+827	7275 (333)	12.8 (0.6)	7.99 (0.07)	H	0.59 (0.04)	1.43 (0.13)	2.0	13.20 (0.10)	0.013
2002−110	4813 (54)	10.1 (0.2)	8.33 (0.02)	He	0.78 (0.01)	8.97 (0.05)	9.1	15.53 (0.03)	0.347
2054−050	4626 (47)	11.8 (1.0)	8.09 (0.12)	He	0.63 (0.08)	8.33 (1.16)	8.7	15.35 (0.17)	1.130
2248+293[j]	5607 (106)	16.6 (1.5)	7.55 (0.16)	H	0.35 (0.07)	1.59 (0.35)	...	13.78 (0.20)	0.122
2251−070	4586 (61)	9.7 (0.4)	8.38 (0.05)	He	0.82 (0.03)	9.68 (0.05)	9.8	15.82 (0.08)	0.254
2316−064	4747 (53)	11.1 (1.3)	8.19 (0.17)	He	0.69 (0.11)	8.58 (1.24)	8.8	15.38 (0.25)	0.046

[a] Total age is cooling age plus $t_{\rm MS}$, where (Wood 1992) $t_{\rm MS} = 10(M_{\rm MS}/M_\odot)^{-2.5}$, and $M_{\rm MS}/M_\odot = 8 \ln_e[(M_{\rm WD}/M_\odot)/0.4]$.

[b] LHS 147: Hα profile implies a low surface gravity and an overluminous star: possible multiple system.

[c] G77−50: Hα profile implies a low surface gravity and an overluminous star: possible multiple system.

[d] G107−70: Known binary: if identical pair, then $M/M_\odot = 0.60$, cooling age = 6.5Gyr, total age = 7.0 Gyr, and $M_{\rm bol} = 14.9$.

[e] LHS 235: Energy distribution best fitted by He-rich model but broad Hα observed.

[f] LHS 239: Low surface gravity implies a large radius and an overluminous star: possible multiple system—if identical pair, then $M/M_\odot = 0.73$, cooling age is 9.2 Gyr, total age is 9.4 Gyr, and $M_{\rm bol} = 16.0$.

[g] LHS 1980: Energy distribution best fitted by an H-rich model: no Hα observed spectrum is noisy.

[h] G195−19: Energy distribution better fitted by an H-rich model: no Hα observed but has broad absorption in blue and is magnetic.

[i] LP 131−66: Low surface gravity implies a large radius and an overluminous star: possible multiple system—if identical pair, then $M/M_\odot = 0.65$, cooling age is 9.0 Gyr, total age is 9.3 Gyr, and $M_{\rm bol} = 16.0$

[j] G128−7: Low surface gravity implies a large radius and an overluminous star: possible multiple system—if identical pair, then $M/M_\odot = 0.65$, cooling age = 4.3 Gyr, total age = 4.6 Gyr, and $M_{\rm bol} = 14.5$

group of stars that are chemically interesting are the carbon-rich DQ and C_2H stars. The former show blue Swan bands, and the latter show what appear to be similar bands shifted slightly to the blue (see, e.g., Fig. 30 of BRL). Schmidt et al. (1995) identified these features as likely to be due to C_2H, the result of the simultaneous presence of hydrogen, helium, and carbon. In this sample there are two DQ stars with helium-dominated atmospheres [Wolf 219 (0341+182) and L879−14 (0435−088)] and two C_2H stars with mixed hydrogen and helium atmospheres [LHS 290 (1043−188) and G225-68 (1633+572)].

Unresolved binaries are an important group in this sample. If the overluminous stars in this sample are, in fact, multiple systems that have been interpreted as single stars, then their radius will be too large and their surface gravity too small, and they will be fainter and older than implied by the single-star interpretation. Candidate unresolved systems are identified in Table 2. To estimate the possible errors in

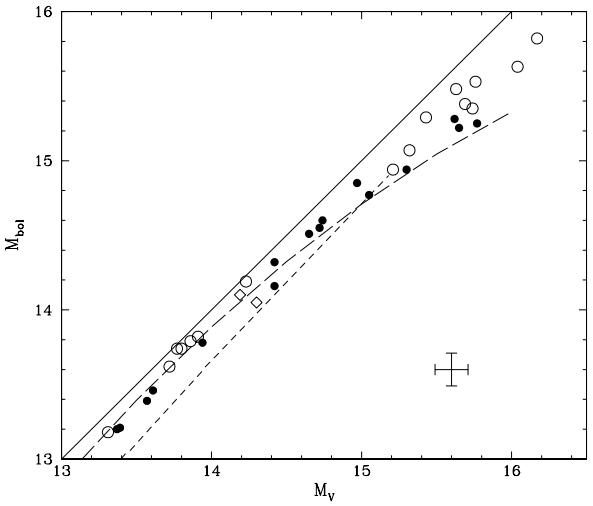

FIG. 1.—M_V against M_{bol}: (*filled circles*) this work for H-rich stars, (*open circles*) this work for He-rich stars, (*open diamonds*) this work for mixed composition stars. The solid line is $M_V = M_{bol}$, or BC = 0. The long-dashed line is the function by LDM for non-DA stars based on blackbody BCs. The short-dashed line is their function for DA stars from hydrogen models available in 1988.

the derived stellar parameters, we treat these objects as a pair of identical stars and derive the new parameters given in the notes at the end of the table. It will be difficult to interpret these systems further unless they can be resolved by, for example, speckle imaging, or if line shifts could be observed spectroscopically.

For this work it is useful to identify the oldest stars in the sample. These have $M_{bol} > 15.5$ ($\log L/L_\odot < -4.3$) and are older than 9 Gyr, based on cooling curves for carbon-core white dwarfs (oxygen-core would reduce the age by ~ 1.5 Gyr). The three that fall into this category are LHS 2673 (1300+263), LHS 483 (2002−110), and LP 701−29 (2251−070). These stars have 4500 K $\leq T_{eff} \leq$ 4800 K. They all have He-rich atmospheres, and so the age is calculated based on "thin" envelopes—"thick" envelopes would reduce the age ~ 1.5 Gyr. They have masses 0.7–0.8 $M/M_\odot$, slightly higher than the mean mass for this sample of 0.68 $M/M_\odot$, as would be expected (more massive white dwarfs evolve from more massive progenitors which reach degeneracy more quickly). There are two other systems that are suspected multiples that may be ~ 9.3 Gyr old: LP 131−66 (1247+550) and LHS 239 (0747+073A, however, the companion appears to be significantly younger). Note that a faint and cool white dwarf is not necessarily old. For example, Ruiz et al. (1995) showed that the extremely faint white dwarf ESO 439−26, with $M_{bol} = 17.1$, is only aged about 7 Gyr. This star is, in fact, massive ($M = 1.2\ M_\odot$, $\log g = 9.0$) and therefore has a very small radius, hence the faintness of the star. Furthermore, crystallization has occurred in this star (crystallization occurs earlier for more massive stars), and it has cooled rapidly, taking only 7 Gyr to cool down to 4500 K.

3.2. *Comparison to LDM*

Finally, before deriving the LF, we compare our stellar properties to those derived by LDM. Our more complete data set has allowed us to be more confident about the dominant chemical composition of the atmospheres of these stars, and our models are both physically superior and are able to cover a wider range of parameters, as compared to those available in 1988. In Table 2 of LDM, the authors presented a selection of cool degenerates with, for that time, reasonably well-determined parameters. They used these stars to investigate bolometric corrections as a function of composition and temperature. There are 18 stars in this table for which we have presented parameters, either in BRL or this work. We find that of these 18, six have had their composition revised (from pure helium to pure hydrogen or in one case mixed hydrogen-helium). Subtracting our T_{eff} values from their values, for these 18 stars, gives an average difference of -365 K $\pm$ 485 K. This is a significant difference, larger than our measurement uncertainties. A comparison of bolometric magnitudes is of more direct relevance to the LF and this work. In LDM the authors derived bolometric magnitudes in two different ways, both of which are plausible, and they argued that these values should bracket the true solution. The two methods used were (1) to use the bolometric corrections calculated from hydrogen atmospheres for the DA stars and from blackbodies for non-DA stars and (2) to assume a mean white dwarf radius which, combined with their derived temperatures, gives luminosity—this latter result was consistent with a zero bolometric correction, that is $M_V = M_{bol}$. Note that the model and blackbody bolometric corrections implied an atypical white dwarf radius. Note also that for the coolest degenerates (stars that are too cool to show Hα), they were forced to assume helium-rich atmospheres. Figure 1 plots M_V against M_{bol}. The filled circles are our results for H-rich stars in this sample, the open circles the He-rich stars, and the open diamonds the mixed composition stars. Only stars with well-determined parallaxes are shown (parallax error < 30%). A typical error bar (due to typical parallax errors of 5%) is shown. The solid line represents $M_V = M_{bol}$ or a zero bolometric correction. The long-dashed line in Figure 1 is the function fitted by LDM for non-DA stars based on blackbody bolometric corrections. The short-dashed line is their function for DA stars based on bolometric corrections from hydrogen models available at that time. It can be seen that the range of M_{bol} values determined by LDM—the region between the solid and dashed lines—do bracket the true solution (*circles* and *diamonds*). However, this range is large, especially at the faint end. Figure 1 shows that the uncertain bolometric corrections available to LDM lead to an uncertainty in $M_{bol} \sim 0.6$ magnitudes at the terminus of the white dwarf sequence. An improvement in the M_{bol} determinations, such as those we have achieved in this work, is crucial in determining the LF turnover and in constraining the disk age, as we show in the following section.

4. DERIVATION OF THE LUMINOSITY FUNCTION

Schmidt (1975) presents a method for deriving a LF from a complete proper-motion selected sample, with known parallaxes and magnitudes. Given that the sample is complete to a lower proper motion limit μ_l and to a faint magnitude limit m_f, there is then a maximum distance r_{max} over which any star can contribute to the sample. This maximum distance is

$$r_{max} = \min\ [p^{-1}(\mu/\mu_l);\ p^{-1}10^{0.2(m_f - m)}]\ , \qquad (3)$$

where p is the stellar parallax, μ its proper motion, and m the apparent magnitude. If the sample is only complete to a certain upper proper-motion limit μ_u and bright magnitude

limit m_b, then there is also a minimum distance

$$r_{\min} = \max\,[p^{-1}(\mu/\mu_u);\ p^{-1}10^{0.2(m_b-m)}]\ . \quad (4)$$

If the sample only covers a fraction of the sky β, then the maximum volume in which a star can contribute is

$$v_{\max} = \tfrac{4}{3}\beta\pi(r^3_{\max} - r^3_{\min})\ . \quad (5)$$

The contribution to the LF from each star is then $1/v_{\max}$, and the LF is calculated by summing the $1/v_{\max}$ values over discrete magnitude intervals. This method is often referred to as the $1/v_{\max}$ method (Schmidt 1968, 1975). The Luyten (1979) survey was limited to declinations greater than $-20°$, and also the galactic plane was avoided, leading to an additional incompleteness of 20%, so $\beta = 0.8 \times 0.671$. For Luyten (1979), $\mu_l = 0\farcs8\ \mathrm{yr}^{-1}$, $\mu_u = 10\farcs0\ \mathrm{yr}^{-1}$, $V_f = 19$ mag, and $V_b = 1$ mag. Hence, for this sample,

$$v_{\max} = 2.249\ [(pr_{\max})^3 - (pr_{\min})^3]/p^3\ . \quad (6)$$

Table 2 gives the $1/v_{\max}$ values for each star in the sample. Clearly the star has a larger contribution to the LF if $v_{\max}$ is small. In practice, this happens for the nearby stars with small proper motion—the star occupies a small volume, and if it were moved (hypothetically) to larger distances, the proper motion would fall below the lower limit and it would not be in the sample. The stars that make the smallest contribution are the stars at large distances with relatively large proper motions.

It is difficult to calculate the error in the LF. LDM adopted the conservative approach that the error in each star's contribution was equal to the size of the contribution itself, and the total error in each magnitude bin is then equal to the square root of the sum of the squares of the contributions. Another approach would be to use the error in the bolometric luminosity to calculate how many stars could be thrown into or out of each magnitude bin, including the effect of unresolved binaries. We have tried both approaches and found that they give similar results (in this work we adopt the LDM approach for consistency). The final derived LF is given in Table 3, based on half-magnitude intervals and derived twice, shifting the bin centers a quarter of a magnitude.

Figure 2 shows various derivations of the cool white dwarf LF. The space density increases to fainter luminosities because of the fact that the cooling rate slows as the white dwarf cools, until crystallization sets in. The peak of the LF at $\log L/L_\odot \sim -4.0$ corresponds to $M_{\rm bol} \sim 14.75$ and $T_{\rm eff} \sim 5300$ K. The dashed line and error bars show the LF derived for hot white dwarfs by LDM, which is based on the volume densities of hot DA white dwarfs published by Fleming, Liebert, & Green (1986). LDM augmented the Fleming et al. (1986) sample by adding the known fraction of hot DB stars, and they also converted the absolute visual magnitudes to bolometric magnitudes (by using bolometric corrections for hot white dwarfs that were reasonably well known, as opposed to the situation with the cool stars). Our cool white dwarf function is shown as filled symbols—the two versions, centered on magnitude bins shifted by a quarter of a magnitude, are shown as circles and squares, with error bars only shown for one set. The point-to-point scatter implied by the two functions gives an idea of binning errors and supports our error estimates. We also show the two functions determined by LDM by using their different techniques for deriving bolometric correction as described in § 3.2 above: the open circles are their results using bolometric corrections calculated from hydrogen atmospheres

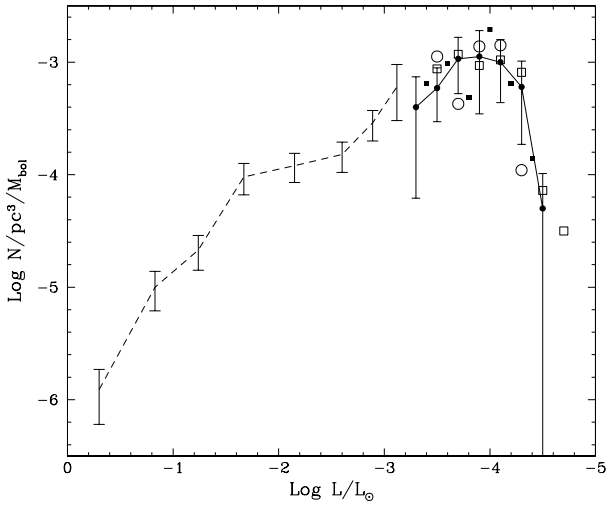

FIG. 2.—Observational LF: (*dashed line*) hot white dwarfs from LDM based on Fleming, Liebert, & Green 1986, (*solid line* and *solid symbols*) this work, (*open symbols*) LDM. See discussion in text.

TABLE 3

LUMINOSITY FUNCTION

$M_{\rm bol}$	Log $L/L_\odot$	Number	Space Density in 0.5 mag Bins (10^{-4} pc^{-3})	Log ϕ Space Density log $\{[\sum (1/v_{\max})]$ mag$^{-1}\}$
13.0	−3.3	4	1.99	−3.40 (+0.27) (−0.81)
13.5	−3.5	5	2.96	−3.23 (+0.18) (−0.30)
14.0	−3.7	8	5.41	−2.97 (+0.19) (−0.31)
14.5	−3.9	6	5.62	−2.95 (+0.13) (−0.51)
15.0	−4.1	10	5.02	−3.00 (+0.20) (−0.36)
15.5	−4.3	7	3.01	−3.22 (+0.23) (−0.51)
16.0	−4.5	1	0.25	−4.30 (+0.31) (−∞)
		Bins Recentered		
13.25.....	−3.4	5	3.21	−3.19 (+0.20) (−0.40)
13.75.....	−3.6	6	4.88	−3.01 (+0.19) (−0.35)
14.25.....	−3.8	5	2.47	−3.31 (+0.20) (−0.36)
14.75.....	−4.0	12	9.75	−2.71 (+0.17) (−0.29)
15.25.....	−4.2	8	3.19	−3.19 (+0.16) (−0.28)
15.75.....	−4.4	3	0.69	−3.86 (+0.21) (−0.44)

for the DA stars and calculated from blackbodies for non-DA stars; the open squares use $M_{bol} = M_V$. (To make the diagram more clear, error bars are only shown on our data set, however each of the LDM datapoints has a similar uncertainty to our set). In most cases the LDM values bracket our solution, as would be expected from Figure 1. However the fact that the bolometric corrections were poorly determined in 1988 leads to a large uncertainty in the space densities (completely independent of counting or binning errors), as shown by the range between the open square and circle symbols at each luminosity. The error is particularly uncertain and particularly important at the faint end, as also demonstrated by Figure 1. Our improved data set and models have enabled us to remove at least 50% of the uncertainty (0.2 dex) in the space densities.

It can be seen that the cool white dwarf LF (a proper motion and magnitude limited sample) agrees well with the hot white dwarf LF (which is limited only in magnitude and color). This gives us some confidence in the level of completeness of the cool-star function. However, the $1/v_{max}$ method allows us to estimate completeness by calculating the mean value of v/v_{max}—the actual volume divided by the maximum volume, which should have a value around 0.5 for a complete sample. Our sample has a mean $v/v_{max} \sim 0.37$, suggesting that it is incomplete. However, the agreement with the hot white dwarf LF implies that the effect on the space densities is not larger than our quoted uncertainties of $\sim 50\%$ or 0.2 dex. The Monte Carlo simulations of the $1/v_{max}$ technique by Wood & Oswalt (1997) indicate that the space densities derived for proper motion and magnitude-limited samples should be corrected upward by about 10% (0.04 dex), but their sample to sample variations are large.

We note in passing that our determination of 3.39×10^{-3} white dwarfs per cubic parsec implies that the total white dwarf mass contribution to the disk is 0.002 $M_\odot/\mathrm{pc}^3$. Thus, the white dwarfs contribute little to the local mass density of the disk (only about 1% of the dynamically estimated mass density). Although modern proper-motion surveys in the southern hemisphere (Ruiz et al. 1993) are finding a higher density of white dwarfs, their contribution to the mass density will remain small.

5. DISCUSSION

Wood (1992) fitted theoretical LFs to the LDM results and obtained an age for the disk of the Galaxy of 8–11 Gyr. He found that 40% of the age uncertainty was due to the observational uncertainty in the bolometric corrections. The uncertainty in age due to unknown white dwarf core composition (carbon or oxygen or a mixture of the two) was ~ 1.5 Gyr. The mass of the outer helium layer was also important—increasing this mass by an order of magnitude decreased the age by ~ 0.75 Gyr. The derived age was much less sensitive to the other inputs of the theoretical LF: star formation rate, initial mass function, initial-final mass relation, and disk inflation. Since 1992, Wood has calculated new evolutionary sequences for white dwarfs (Wood 1995); these new sequences have mixed C/O cores, thicker surface layers, and new opacities. Fitting these theoretical LF to the earlier LDM results would imply a younger age for the disk of the Galaxy of 7–9 Gyr.

Oswalt et al. (1996) fitted these new models to a different observational LF, one based on a sample of white dwarfs in binaries. Those authors determined an older age for the disk of ~ 9.5 Gyr. Converting the observational LF in Figure 1 of their paper from $\Delta \log L/L_\odot$ to ΔM_{bol} and comparing to our function (Fig. 2) show that the two functions are very similar in the region, $-2 > \log L/L_\odot > -3.5$. However, their peak value at $\log L/L_\odot \sim -4.0$ is about 40% (0.15 dex) higher than ours, and their final point at $\log L/L_\odot = -4.5$ is about 20 times higher than ours, or 1.2 dex. This leads them to derive a mass density of white dwarfs that is twice our value, and their high last data point implies an older age than that implied by our sample. Although the difference in the peak value of 0.15 dex is within the errors of both samples, the last data points (the points that constrain the age) are incompatible. We feel that Oswalt et al. (1996) have probably underestimated their errors for the three stars in this last bin for the following reason: the luminosities are derived from $V-I$ color and optical spectra alone, with the assumption $M_{WD} = 0.6\,M_\odot$. Optical data alone is insufficient to determine reliably chemical composition for the coolest stars (star that may be too cool to show Hα), and Figure 10 of BRL, for example, shows that temperatures derived based on $V-I \sim 1.3$ for pure hydrogen and pure helium compositions differ by around 10%, which imply luminosities differing by 40% (or 0.15 dex). Furthermore, obtaining accurate $V-I$ photometry of close red dwarf/white dwarf pairs, such as the three faintest stars in their sample, is very difficult. One of these three stars [LHS 290 (1043−188)] is also in our sample, and we were not able to determine a meaningful I magnitude for this star due to the close red dwarf. Our $BVRJHK$ data imply a $V-I$ more blue by ~ 0.5 mag than quoted by Oswalt et al. (1996), and we determined that the star is more luminous by a factor of 4. Although this star contributes very little to the space density of their last bin, we expect that the two other stars (which are fainter and have companions at similar distances) have similarly compromised $V-I$ and hence luminosities. Therefore, we suggest that the Oswalt et al. (1996) final data point is not well determined and that they have not constrained the age of the disk.

In Figure 3 we fitted our LF, based on the LDM sample, to the new sequences by Wood (1995). The resulting age for the disk—time since star formation began—is 8 ± 0.5 Gyr, which should be representative of an annulus through the

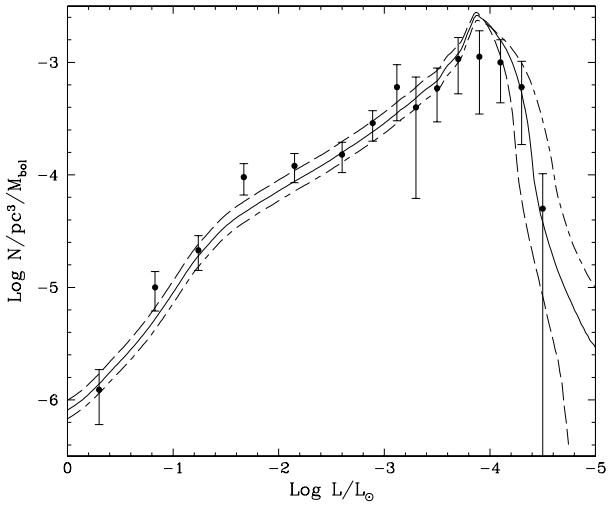

FIG. 3.—Observational LF from this work fitted to theoretical sequences by Wood (1995): (*solid line*) 8 Gyr, (*dashed line*) 7 Gyr, and (*dot–dashed line*) 9 Gyr.

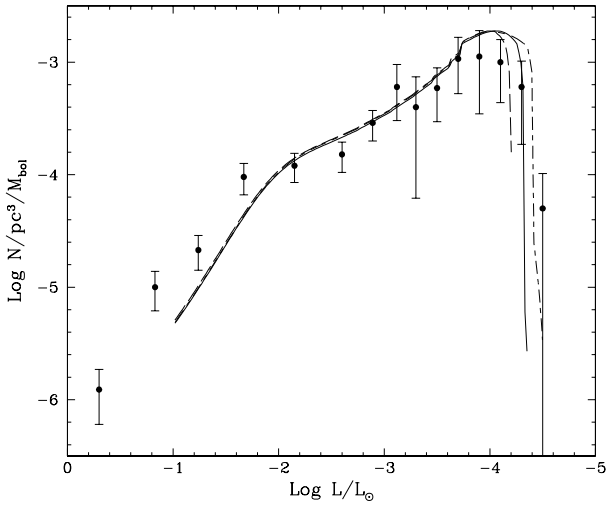

FIG. 4.—Observational LF from this work fitted to theoretical sequences by Hernanz et al. (1994): (*solid line*) 9 Gyr, (*dashed line*) 8 Gyr, (*dot-dashed line*) 10 Gyr.

disk at about the distance of the sun. Systematic uncertainties due to core composition and mass of the outer layers amount to ± 1.5 Gyr (Wood 1992). It is these systematic effects that lead to our LF age being younger than some of the stellar ages given in Table 2. The evolutionary models used to derive the ages in Table 2 (discussed in §§ 3 and 3.1) were for carbon core composition and for a mixture of thick and thin envelopes. The recent theoretical LFs used to derive the disk age use a mixed C/O core composition and thick envelopes only—both these lead to younger ages.

There is a further age uncertainty related to the white dwarf core, as described by Hernanz et al. (1994). As a white dwarf cools, the core will eventually go through a phase transition from the liquid state to the solid state, which is known as crystallization (e.g., Lamb & Van Horn 1975). This phase transition happens earlier for more massive white dwarfs, and it is likely to be important for the very coolest stars. Hernanz et al. (1994) point out that if a white dwarf has a carbon/oxygen core, then the elements might separate on crystallization, releasing gravitational energy and delaying the cooling of the white dwarf by ~ 2 Gyr. Figure 4 fitted their theoretical LFs, which include this separation process, to our observational LF. These Hernanz et al. (1994) models already included some C/O stratification from the onset of white dwarf evolution (if all stratification occurred on crystallization, then the age would increase), but they also have "thin" envelopes (if the envelope mass is increased, which better matches current estimates, then the age would decrease). Fitting these models to our result implies an age for the disk of around 9 Gyr.

In summary, we have greatly improved the determination of the observational LF for cool white dwarfs. Fitting it to current theoretical cooling sequences for white dwarfs implies an age for the disk of the Galaxy of 8 ± 1.5 Gyr, where most of the uncertainty is now in the core composition, the effect of separation on crystallization, and the unknown mass of the outer envelope. We are confident that this sample, drawn from the Luyten Half-Second Catalog (Luyten 1979), is not severely incomplete because of the good agreement with other samples. There is the worry that small number statistics at the faint end of the LF may lead to erroneous conclusions, but although new cool white dwarfs are being found in, for example, proper-motion surveys in the southern hemisphere, none of these are older than those in this sample (see, e.g., BRL). Finally, the Monte Carlo simulations of the white dwarf LF by Wood & Oswalt (1997) show that for a sample like the LDM sample, the error in the derived age due to sample incompletness is ~ 1 Gyr. Usually, but not always, their artificial sample implies an age that is younger than the true age. By including these simulated effects, the *total* uncertainty in our derived age would be ~ 2 Gyr. It would clearly be desirable to increase the size of the observational sample to constrain better the turnover of the function (currently determined by 1–3 stars). Wood & Oswalt's (1997) study implies that if the sample size could be increased to 200, then the age would be constrained to ~ 0.5 Gyr, not including the uncertainties in cooling theory due to core composition, etc. Various groups are working on increasing the cool white dwarf sample size.

Although an age of 8 ± 1.5 Gyr for the local region of the Galaxy may appear young, it is interesting to note that recent determinations of the ages of globular clusters are reducing cluster ages from 14–18 Gyr to 11–12 Gyr (D'Antona, Caloi, & Mazzitelli 1997) and recent estimates of Hubble's constant puts the expansion age of the universe to a young 8–11 Gyr (Mould et al. 1995). D'Antona, Caloi, & Mazzitelli (1997) point out that these results are compatible if Hubble's constant is less than 65 km s^{-1} Mpc^{-1} and the cosmic density is slightly lower than required for closure ($\Omega \leq 0.7$). Recent *Hipparcos* results for metal-poor stars (Reid 1997) and for Cepheid variables (Feast & Catchpole 1997) also appear to support a younger age for the globular clusters and the universe.

We are very grateful to the staff at CTIO, KPNO, IRTF, and UKIRT for their assistance in obtaining the data presented in this paper. UKIRT, the United Kingdom Infrared Telescope, is operated by the Joint Astronomy Centre on behalf of the UK Particle Physics and Astronomy Research Council. The IRTF, the NASA Infrared Telescope Facility, is operated by the University of Hawaii, under contract to NASA. This work has been supported in part by NSERC Canada, by the fund FCAR (Québec), by the FONDECYT grant 1950588, by a Catedra Presidencial en Cienias 1996 award, by NSF grant 93-15372, and by a Chrétien International Research grant. We are grateful to the referees M. Wood and T. Oswalt for a careful review of the manuscript.

REFERENCES

Bergeron, P., Ruiz, M. T., & Leggett, S. K. 1997, ApJS, 108, 339 (BRL)
Bergeron, P., Saffer, R. A., & Liebert, J. 1992, ApJ, 394, 228
Bergeron, P., Saumon, D., & Wesemael, F. 1995, ApJ, 443, 764
Bessell, M. S., & Weis, E. W. 1987, PASP, 99, 642
Dahn, C. C., Hintzen, P. M., Liebert, J. W., Stockman, H. S., & Spinrad, H. 1978, ApJ, 219, 979
D'Antona, F., Caloi, V., & Mazzitelli, I. 1997, ApJ, 477, 519
Elias, J. H., Frogel, J. A., Matthews, K., & Neugebauer, G. 1982, AJ, 87, 1029
Feast, M. W., & Catchpole, R. M. 1997, MNRAS, 286, L1
Fleming, T. A., Liebert, J., & Green, R. F. 1986, ApJ, 308, 176
Hernanz, M., García-Berro, E., Isern, J., Mochkovitch, R., Segretain, L., & Chabrier, G. 1994, ApJ, 434, 652
Iben, Jr., I., & Laughlin, G. 1989, ApJ, 341, 312
Lamb, D. Q., & Van Horn, H. M. 1975, ApJ, 200, 306
Liebert, J., Dahn, C. C., & Monet, D. G. 1988, ApJ, 332, 891 (LDM)
Liebert, J., Dahn, C. C., & Monet, D. G., 1989, in IAU Colloq. 114, White Dwarfs, ed. G. Wegner (Berlin: Springer), 15

Luyten, W. J. 1979, The LHS Catalogue, 2d Ed., (Minneapolis: Univ. Minnesota)
Monet, D. G., Dahn, C. C., Vrba, F. J., Harris, H. C., Pier, J. R., Luginbuhl, C. B., & Ables, H. D. 1992, AJ, 103, 638
Mould, J., et al. 1995, ApJ, 449, 413
Oswalt, T. D., Smith, J. A., Wood, M. A., & Hintzen, P. 1996, Nature, 382, 692
Reid, I. N. 1997, AJ, 114, 161
Ruiz, M. T., Takamiya, M. Y., Mendez, R., Maza, J., & Wishnjewsky, M. 1993, AJ, 106, 2575
Ruiz, M. T., Bergeron, P., Leggett, S. K., & Anguita, C. 1997, ApJ, 455, L159
Salaris, M., Hernanz, M., Isern, J., Dominguez, I., García-Berro, E., & Mochkovitch, R. 1996, in Proc. of the 10th European Workshop on White Dwarfs, White Dwarfs, ed. J. Isern, M. Hernanz, & E. García-Berro (Dordrecht: Kluwer), 27
Schmidt, G. D., Bergeron, P., & Fegley, Jr., B. 1995, ApJ, 443, 274
Schmidt, G. D., & Smith, P. S. 1995, ApJ, 448, 305
Schmidt, M. 1968, ApJ, 151, 393
———. 1975, ApJ, 202, 22
Sion, E. M., Kenyon, S. J., & Aannestad, P. A. 1990, ApJ, 72, 707
Wesemael, F., Greenstein, J. L., Liebert, J., Lamontagne, R., Fontaine, G., Bergeron, P., & Glaspey, J. W. 1993, PASP, 105, 761
Winget, D. E., et al. 1987, ApJ, 315, L77
Wood, M. A. 1990, Ph.D. thesis, Univ. Texas at Austin
———. 1992, ApJ, 386, 539
———. 1995, in Proc. of the 9th European Workshop on White Dwarfs, NATO ASI Ser., ed. D. Koester & K. Werner (Berlin: Springer), 41
Wood, M. A., & Oswalt, T. D. 1997, ApJ, in press
van Altena, W. F., Lee, J. T., & Hoffleit, E. D. 1994, The General Catalogue of Trigonometric Parallaxes (New Haven: Yale Univ. Observatory)